2021 Annual Report #20001

Nonlinear seismic waves with applications to strong ground motions

Principal Investigator: Norman H. Sleep

March 01, 2021

We continued our purposed work on nonlinear propagation of strong seismic waves, which are central to the SCEC purview of strong ground motions. Nonlinear failure likely occurs within the shallow (meters to tens of meters) depths within the well-known geotechnical layer. The near-field velocity pulse may trigger near-fault failure in the rock mass to a few kilometers depth. (Long-period (~3 s) surface waves also attenuate nonlinearly at hundreds of meters depth.) We completed study on the 2002 Denali mainshock, which was recorded by station PS10, where both types of failure are plausible [1]. We also finished a limited field project related to the Ridgecrest earthquake sequence [2]. We collaborated on a SCEC Community review of fragile geological features [3]. We unsuccessfully examined records from the Ridgecrest mainshock at stations CLC and CCC for nonlinear effects. We have now examined available strong motion digital seismograms for nonlinear effects. We had already examined shallow (hundreds of meters) *S*-wave well logs for damage in ambient rock for paleoseismology. We continue to work on immediate *P*-wave triggered events from the Parkfield mainshock.

Our delays from the COVID-19 pandemic continue. We still have no access to our offices nor multiprocessor computers. The P.I. has been unable to return our Ridgecrest field sites. He likely contracted COVID-19 around March 15, 2020. Testing was then available only for the direly ill and a positive test would not have affected recommended treatment. The test site was a prime place to become positive if not already infected. He did not become dangerously ill, but by the time he was well enough to travel, things were locked down. Now two winters with some rain have passed. He will still try to get back to Ridgecrest. We were unable to continue our field work related to strong shaking from the end-Cretaceous asteroid impact in Montana.

Given these situations, the P.I. announced retirement from Stanford on March 31 2021. This is our final SCEC project and report. We thank SCEC for its continued support. We feel that our observational and modeling work on nonlinear seismic waves has been useful to the SCEC community and has alerted the community to the need for three-dimensional numerical models. We have also made progress on the physics of fault planes and on the nonlinear physics of rock and soil masses. The P.I. plans to remain active in the SCEC community.

Paleoseismology field work related to Ridgecrest earthquakes. Chance observations by the P.I. on his return from the 2019 SCEC meeting to Menlo Park resulted in a field project. He had planned to visit the fallen pinnacle at Trona and thus took Trona road from US395 to SR178. There are nice exposures of spheroidal granite knobs at Wagon Wheel Staging Area (35.573°N, 117.551°, 3390 m elevation). The P.I. stopped to search for fallen precarious rocks. Rather, he found numerous examples where low-lying boulders on the grus were mildly displaced within their sockets during the events (Figure 1). He documented the examples and then contacted the geologists working in the area. Susan Hough (USGS) examined the area and found an example of a semi-precarious rock that was displaced but not toppled. She confirmed that no boulders were displaced near a seismic station that recorded modest shaking. We worked together [2]. Our low-

lying boulders are distinct from rock damage associated with frost and weathering at the top of the knobs. Randall Jibson pointed out this confounding effect to us.

Mildly displaced rocks have not received much attention [e.g., 4-5]. We developed simple analytical and numerical models for low-lying and semi-precarious rocks. Low-lying rocks slide when the dynamic forces exceed frictional resistance at the base. The grus does not significantly resist plowing by the edge of the rock and we confirmed with a small slab that the sockets have little tensional strength. Semi-precarious rocks begin to tilt when their instantaneous center of gravity becomes outside their base. In both cases, full (horizontal and vertical) dynamic accelerations are between 0.5 and 1 *g*. This shaking is somewhat higher for both the large foreshock and the mainshock than predicted by Shake Maps. We suspect that the damage was caused by the large foreshock; it has the closest fault rupture. Note that there were no known tent or RV campers at Wagon Wheel Staging Area at the time of the earthquakes. The area is typically unoccupied at the time owing to extreme heat and no camping permits are required. A shaken or tipped RV would not have escaped press attention and would have brought geologists immediately to this site.

More importantly than finding a site of strong shaking, we recognized a potentially applicable paleoseismic method (Figure 1). Organic debris of the year including twigs, seeds, and leaves were already starting to enter the gaps beneath the sockets and above the rocks in September 2019. Small animals may enter the gaps and become entombed. This datable horizon should underneath the boulder until it is obscured by bioturbation. In contrast, the surface gaps are likely already obscured by hard rains. The P.I. became ill with COVID-19 in mid-March 2020 and travel to Ridgecrest is now locked down. Calibration for paleoseismology seems feasible but would require industrial equipment to lift boulders and scientists qualified to do careful sampling. The locations of the 1992 Landers event and the 1872 Owens Valley event are well known. There are plenty of granite knobs with boulders resting on grus in these regions. A considerable part of our SCEC efforts have been related to recognizing nonstandard fragile geological features for future study.

Paleoseismology: End-Cretaceous impact. As outreach, we have collaborated with Peter Olds of Alameda College and taken junior college students to search for faults triggered by the end Cretaceous asteroid impact. It is no surprise that the extreme seismic waves from this event triggered small earthquakes. We immediately found two exposures of a fault that appeared to have slipped once in the immediate aftermath of the impact at well-known exposures (one behind the Iridum layer sign in the State Park) near Trinidad CO [6]. This fault did not slip again over the subsequent ~66 Ma. However, we found other faults that slipped within tens of millennia after the impact in New Mexico (behind Iridium Layer sign at Goat Hill, Raton) and Jordan Montana but have not slipped since. An attractive hypothesis is that the impact triggered a very large number of huge intraplate events and it took tens of millennia for global intraplate stress to return to normal. With the help of paleontologist Greg Wilson, we searched the Jordan area for more faults in 2019. Many faults cut the section well above the impact horizon. (The paleontologists measure up or down from the impact layer. Faults with centimeters to a few meters of throw do not hinder their work and had not been systematically studied.) Our previously found faults that cut only slightly above the impact horizon are thus unrepresentative. There is also a sampling bias as offset of the K-Pg layer within the Z Coal in the Jordan area can be seen at a distance. Our data are thus inconsistent with a simple hypothesis that the impact transiently reset the tectonic stress in the Jordan area.

Shallow to moderate-depth nonlinear seismology. It is well-known that strong body waves may bring the shallow (geotechnical) subsurface into nonlinear failure. Energy is dissipated from the

waves and the overall intensity of surface shaking is reduced. We have examined records from the 2002 Denali mainshock at station PS10 [1] and the 1992 Landers earthquake at station LUC [1]. Simple scaling relationships arise if a near-surface low-velocity layer exists. (1) The waves refract into nearly vertical paths. Analytical and nonlinear numerical modeling become simple for vertically propagating waves within a laterally stratified medium. Inelastic failure may be represented as horizonal shear on horizontal planes. (2) The Coulomb ratio of dynamic stress to lithostatic stress from *S* waves is the normalized acceleration in *g*'s. A Coulomb frictional material is predicted to fail when the normalized dynamic acceleration exceeds the effective coefficient of friction. Dynamic (resolved) horizontal acceleration is predicted to clip in *g*'s at the effective coefficient of friction. This process occurs within the ground and is distinct from instrumental clipping. (3) For plausibility, a similar relationship applies for vertical *P* waves. The ratio of vertical dynamic stress to lithostatic stress is the normalized vertical acceleration. Strong downward accelerations around 1 *g* should bring the shallow surface into tensional failure. Downward acceleration thus is predicted to clip around 1 *g*. This effect has been observed during large earthquakes [7-11]. *P* waves were relatively feeble at station PS10 during the Denali mainshock [1]. Thus, considering the event as having only vertical *S* waves provides a reasonable approximation. The observed horizontal signal is circularly polarized for about 1/3 of a cycle and clipped at ~0.35 *g*. An effective coefficient of friction of ~0.35 is acceptable for the water-saturated gravel that underlies PS10. The result is thus consistent with the hypothesis of frictional failure.

The seismological community, including journal reviewers, have become highly skeptical of scaling relationships in general and our use of a nonstandard engineering rheology (Coulomb friction) for gravel in particular. We have confirmed our scaling inferences with one-dimensional numerical models [1]. We recognize that three-dimensional numerical methods are available [12-15]. Our scaling relationships aid in planning and understanding complicated numerical efforts. We provide candidate rheologies. We recognize that it is unproductive to produce very complicated shallow scaling relationships for real situations that can better be addressed numerically.

Our work still illustrates features that may occur in future large earthquakes. The scaling relationships and one-dimensional models are guides for future three-dimensional calculations, for example, if nonlinear failure occurs within a dense borehole and surface array. Hence, we examined records for the 2019 Ridgecrest strong foreshock and mainshock. The water table is likely deep beneath stations CLC and CCC, which experienced the strongest shaking. Accelerations from body waves appear to have been too feeble to have caused frictional failure. There is no apparent clipping.

We searched nonlinear failure within crystalline rock beneath station PS10 during the Denali earthquake [1]. The process may be represented more quantitatively by three-dimensional nonlinear dynamic numerical models [12-15], but there were no other stations near PS10. The PS10 recorder was "one and done" and only recorded aftershocks for tens of seconds. A new PS10 was installed by the USGS at a nearby site and recorded aftershocks from one week to two weeks after the event. BSSA reviewers insisted that we access these data. We were able to track them down. USGS Golden agreed to preserve these data that were about to be jettisoned and to provide them to an archiving service. We were unable to resolve healing of damage within the shallow gravel or the uppermost crystalline rock from this data [1]. Our methods may be useful for future well recorded events.

To the first order, the near-field pulse imposed dynamic strains on shallower more compliant rocks. The peak dynamic strain scales with the peak ground velocity divided by the rupture

velocity. The dynamic stress scales with the strain times the shear modulus. We found that the uppermost stiff crystalline rock at ~100 m depth beneath gravel was most prone to failure and that failure may have occurred down to ~2 km depth. We suspect a deep high-frequency (several Hz) nonlinear effect beneath PS10. Cracks in the crystalline rock do not distinguish between remote sources of stress. Here, low-frequency (less than ~1 Hz) dynamic stresses likely brought the subsurface into nonlinear failure. High-frequency *S* waves passing through the failed region should also nonlinearly attenuate. High frequency *S* waves were in fact weak at PS10 during the near-field pulse. We suspect a similar effect during strong shaking at LUC during the Landers earthquake.

We note puzzling behavior occurred at PS10: (1) The weak *S* waves persisted for over 10 s after the near-field pulse had passed. Perhaps, the *S* waves nonlinearly interacted with inelastic strain rates from the initial rapid healing of the damage. (2) The *S* waves were strongly depleted in high frequencies with an apparent *Q* of ~20. Simple frictional, plastic, and viscous rheologies do not preferentially suppress high frequencies in this manner. A linear rheology represented by multiple Maxwell spring and dashpots combinations acting in parallel can produce a nearly constant *Q*. The effective viscosity (represented by a dashpot) and hence Maxwell times are expected to vary among stress concentrations in a highly nonlinear material. From simple crack theory, the elastic compliance of a crack depends on its long/short aspect ratio. The inelastic compliance depends on this ratio to a high power. Furthermore, highly compliant cracks close elastically or rapidly inelastically and thus cease to be present rapidly after the damage. We do not feel that complicated scaling relationships would provide insight beyond these banalities. We are unable to compute full numerical models, but we have pointed out the situation to the modelers.

Immediately triggered "spot-fire" events during the Parkfield mainshock. We plan to continue our work on the 2004 Parkfield earthquake, but we are currently delayed by the pandemic. We will continue to work with William Ellsworth of Stanford. Basically, the rupture front of the mainshock propagated at less than the shear-wave velocity. However, *P* waves outran the rupture front and may have triggered modest (Magnitude ~3.5) "spot-fire" earthquakes that occurred between the arrival of the P wave and the arrival of the S wave on the fault plane. (The kinematic analogy is to spot fires caused by blown firebrands ahead of the main front of a forest fire.) The Parkfield earthquake then did not evolve into full supershear rupture. We have been searching records from the Pilot Hole array for high-frequency *S* waves from such spot-fire events. Surface stations were too noisy to be useful. We have found candidate arrivals. From comparison with known aftershocks, the putative magnitudes were approximately 3.5.

The subsurface structure beneath Parkfield, however, is complicated. High-frequency shear arrivals could be converted phases, for example, reflections from the fault plane. At the time of the mainshock only about 7 stations were working in the borehole. We can determine moveout of phases and separate upcoming and downgoing waves. The curvature of the wave fronts is not well resolved. We have candidate events that need to be distinguished from converted phases. We are examining records of small earthquakes that were recorded when the full array was still present. We can recognize converted phases of comparison with the mainshock records. There were small earthquakes both near the hypocenter of the mainshock and near the locations of putative spot-fire events. Confirming spot-fire events will show that stress concentrations exist on the fault plane. Not finding any will still provide methods for future studies.

Nonlinear near-surface interaction of the rupture tip with high-frequency *S* waves. We proposed to continue work on the interaction of strong high-frequency *S* waves with the tip of shallow dynamic rupture. Basically, the high-frequency *S* waves arrive at the surface before the

rupture tip during a strike-slip earthquake. The rupture tip enters the shallow region of nonlinear failure from the *S* waves. Stresses from the tip interact with those from the S waves. Failure occurs over a finite width at the surface and the static displacement is distributed over this width. Nevitt et al. [16] presented quasi-static models of such surface rupture.

We had planned antiplane-strain numerical models, which will confirm the basic kinematics and dynamics of the process. We will try to continue. However, the rupture tip propagates laterally when it first encounters the surface. The initial slip on the rupture may foreordain the subsequent rupture. Vagaries in the rupture propagation velocity may cause the surface tip to locally propagate antithetically to the macroscopic rupture direction. Rupture tips may collide and produce overlapping crack features, which are observed at Ridgecrest. That is, the process is fully three-dimensional and high-resolution nonlinear numerical models are needed. We plan to alert modelers. The antiplane modeling will then unnecessary.

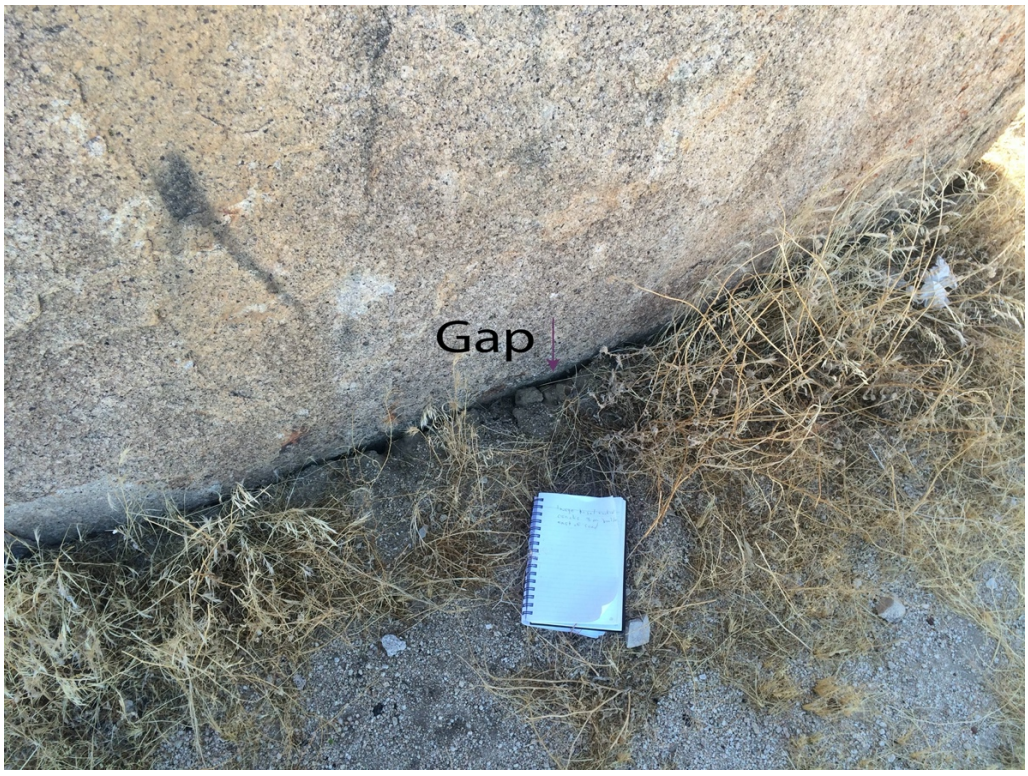

Figure 1. Example mildly displaced rock from Wagon Wheel Staging Area that was affected by Ridgecrest earthquakes. Organic material is already entering the gap between the rock and its socket. We have archived bursts of our photos with location, facing direction, and time metadata. The field sites thus may be revisited in the future to appraise the potential for paleoseismology. We expect rains have already filled the gap with debris including some organic material of the year. There may also be preserved information that relates to the season of the earthquake and perhaps wet or dry decade. Earthquakes with similar ^{14}C ages then can be further correlated or dis-correlated. Spheroidal granite boulders are very common in semiarid regions of California.

References

[1] Sleep, N. H., & Liu, T. (2020). Nonlinear suppression of high-frequency S waves by the nearfield velocity pulse with reference to the 2002 Denali earthquake. *Journal of Geophysical Research: Solid Earth*. SCEC Contribution 9959

[2] Sleep, N. H. and S. E. Hough (2020) Mild displacements of boulders during the 2019 Ridgecrest Earthquakes. *Bulletin of the Seismological Society of America*, *accepted*. SCEC Contribution 10060.

[3] Stirling, M. W., M. E. Oskin, J. R. Arrowsmith, A. H. Rood, C. A. Goulet, L. Grant Ludwig, T. R. King, A. Kottke, J. C. Lozos, C. M. Madugo, et al. (inxluding N. H. Sleep) (2020). Evaluation of Seismic Hazard Models with Fragile Geologic Features, Seismol. Res. Lett. XX, 1–11, doi: 10.1785/0220200197. SCEC Contribution 10777

[4] Haff, P. K. (2005), Response of desert pavement to seismic shaking, Hector Mine earthquake, California, 1999, J. Geophys. Res., 110, F02006, doi:10.1029/2003JF000054.

[5] Sylvester, A. G., K. C. Burmeister, and W. S. Wise 524 (2002) Faulting and Effects of Associated Shaking at Pisgah Crater Volcano Caused by the 16 October 1999 Hector Mine Earthquake (M_w 7.1), Central Mojave Desert, California. Bulletin of the Seismological Society of America; 92 (4): 1333–1340. doi: https://doi.org/10.1785/0120000921

[6] Sleep, N. H. and E. P. Olds (2018) Remote Faulting Triggered by Strong Seismic Waves from the Cretaceous–Paleogene Asteroid Impact. Seismological Research Letters; 89(2A): 570–576. doi.org/10.1785/0220170223. SCEC contribution number 7996.

[7] Aoi, S., T. Kunugi, and H. Fujiwara (2008) Trampoline effect in extreme ground motions. Science, 332, 727-730.

[8] Yamada, M., J. Mori, and T. Heaton (2009) The slapdown phase in high acceleration records of large earthquakes. Seismol. Res. Lett., 80(4), 559-564.

[9] Tobita, T., S. Iai, and T. Iwata (2010) Numerical analysis of near-field asymmetric vertical motion. Bull. Seismol. Soc. Am., 100(4), 1456–1469

[10] Kinoshita, S. (2011) A Stochastic Approach for Evaluating the Nonlinear Dynamics of Vertical Motion Recorded at the IWTH25 Site for the 2008Mw 6.9 Iwate–Miyagi Inland Earthquake. Bull Seismol. Soc. Am., 101, 2955-2966.

[11] Bradley, B. A., and M. Cubrinovski (2011) Near-source ground motions observed in the 22 February 2011 Christchurch earthquake. Seismol. Res. Lett., 82(6), 853-865.

[12] Wang, Y., Day, S. M., & Denolle, M. A. (2019). Geometric controls on pulse-like rupture in a dynamic model of the 2015 Gorkha earthquake. Journal of Geophysical Research: Solid Earth, 124, 1544–1568. https://doi.org/10.1029/2018JB016602.

[13] Roten, D., Y. Cui, K. Olsen, S. Day, K. Withers, W. Savran, W. Peng, and D. Mu (2016), High-frequency nonlinear earthquake simulations on petascale heterogeneous supercomputers, paper presented at ACM/IEEE International Conference for High Performance Computing, Networking, Storage and Analysis (SC'16), pp. 957–968, IEEE Press, Salt Lake City, Utah, 13–18 Nov.

[14] Roten, D., K. Olsen, Y. Cui, and S. Day (2017a), Quantification of fault zone plasticity effects with spontaneous rupture simulations, Pure Appl. Geophys., 1–23, doi:10.1007/s00024-0171466-5.

[15] Roten, D., K. B. Olsen, and S. M. Day (2017b), Off-fault deformations and shallow slip deficit from dynamic rupture simulations with fault zone plasticity, Geophys. Res. Lett., 44, 7733– 7742, doi:10.1002/2017GL074323.
[16] Nevitt, J. M., Brooks, B. A., Catchings, R. D., Goldman, M. R., Ericksen, T. L., & Glennie, C. L. (2020). Mechanics of near-field deformation during co-and post-seismic shallow fault slip. *Scientific Reports*, *10*(1), 1-13.